A&A 474, 521–527 (2007)
DOI: 10.1051/0004-6361:20078246

Astronomy & Astrophysics

Possible gas-phase syntheses for seven neutral molecules studied recently with the Green Bank Telescope⋆

D. Quan[1] and E. Herbst[2]

[1] Chemical Physics Program, The Ohio State University, Columbus, Ohio 43210, USA
e-mail: herbst@mps.ohio-state.edu
[2] Departments of Physics, Chemistry and Astronomy, The Ohio State University, Columbus, OH 43210, USA

Received 9 July 2007 / Accepted 17 August 2007

ABSTRACT

Aims. With the Green Bank telescope (GBT), seven neutral molecules have been newly detected or confirmed towards either the cold interstellar core TMC-1 or the hot core source Sgr B2(N) within the last 1–2 years. Towards TMC-1, the new molecules seen are cyanoallene (CH_2CCHCN) and methyl triacetylene (CH_3C_6H) while methyl cyanoacetylene (CH_3CCCN) and methyl cyanodiacetylene (CH_3C_5N) were confirmed. Towards Sgr B2(N), the three newly detected molecules are cyclopropenone (c-C_3H_2O), ketenimine (CH_2CNH), and acetamide (CH_3CONH_2); these are mainly seen in absorption and are primarily located in an envelope around the hot core. In this work, we report a detailed study of the gas-phase chemistry of all seven molecules.
Methods. Starting with our updated gas-phase chemical reaction network osu.01.2007, we added formation and depletion reactions to treat the chemistry of each of the seven molecules. Some of these were already in our network but with incomplete chemistry, while most were not in the network at all prior to this work. We assumed the standard physical conditions for TMC-1 and assumed that these also hold for the envelope around Sgr B2(N). Standard pseudo-time-dependent calculations were run for each source.
Results. For TMC-1, we reproduced the observed fractional abundances of three detected molecules at early times of 10^{5-6} yr and came close to reproducing a fourth. For the halo surrounding Sgr B2(N), our results are more ambiguous: only for ketenimine were we able to match the observed abundance very well.

Key words. ISM: abundances – ISM: molecules – molecular processes

1. Introduction

In 2006, detections of seven interstellar molecules with the 100-m Green Bank Telescope (GBT) were reported. Towards the cold core TMC-1, two new molecules – cyanoallene (CH_2CCHCN) and methyl triacetylene (CH_3C_6H) – were detected and two species – methyl cyanoacetylene (CH_3CCCN) and methyl cyanodiacetylene (CH_3C_5N) – confirmed. Towards the hot-core source Sgr B2(N) or, more accurately, its environs, three new molecules were seen: cyclopropenone (c-C_3H_2O), ketenimine (CH_2CNH), and acetamide (CH_3CONH_2). These molecules supplement the earlier detection by Hollis et al. (2004) of propenal and propanal towards Sgr B2(N).

The new molecules detected in TMC-1 are analogous to those previously seen in this exceptional source for unsaturated organic molecules. Lovas et al. (2006a) identified cyanoallene (CH_2CCHCN), an isomer of methyl cyanoacetylene (CH_3CCCN), and also confirmed the existence of the latter. Cyanoallene was found to be the more abundant species, with a column density of 2×10^{12} cm^{-2} compared with that of 4.5×10^{11} cm^{-2} for methyl cyanoacetylene. A similar observation was reported with the use of the 100-m Effelsberg telescope (Chin et al. 2006). The formation mechanism of methyl cyanoacetylene has been discussed by a variety of authors. Schwahn et al. (1986) suggested an ion-molecule synthesis starting with the formation of protonated methyl cyanoacetylene via the radiative association of CH_3^+ and cyanoacetylene (HCCCN) and the subsequent formation of CH_3CCCN by dissociative recombination with electrons. On the other hand, Balucani et al. (2002) showed that the neutral-radical reactions between C_3H_4 in its isomeric forms allene (H_2CCCH_2) and methyl acetylene (CH_3CCH) and the CN radical react to produce all three isomers of C_4H_3N: methyl cyanoacetylene, cyanoallene, and 3-cyano methylacetylene ($HCCCH_2CN$). Although ion-molecule routes to methyl cyanoacetylene are in the two current major networks, RATE06 and osu.01.2007 (http://www.udfa.net/; http://www.physics.ohio-state.edu/~eric/research.html), the neutral-radical synthesis appears to have been omitted. The next member of the methyl cyanopolyyne family ($CH_3(CC)_nCN$), methyl cyanodiacetylene (CH_3C_5N), was recently confirmed to be present in TMC-1 with a column density of 7.4×10^{11} cm^{-2} (Remijan et al. 2006; Snyder et al. 2006); the original detection had been made much earlier (Snyder et al. 1984). This species is present in the two main chemical networks; its synthesis is once again limited to ion-molecule processes. The methyl polyynes ($CH_3C_{2n}H$) are another family in TMC-1, and the largest member of this group – methyl triacetylene (CH_3C_6H) – has also been detected recently (Remijan et al. 2006) with a column density of 3.1×10^{12} cm^{-2} although some evidence for this species had been obtained much earlier by Snyder et al. (1984). This species is also in the two networks, where it is produced solely by ion-molecule chemistry. In fact, the computed abundance with an older network of ours, osu.2003, is much too low (Snyder et al. 2006).

⋆ Table 2 is only available in electronic form at http://www.aanda.org

The galactic center source Sgr B2(N) is the site for many discoveries of interstellar molecules, but the three new species reported are of interest in that much of their spectral transitions are in absorption towards the source and two probably derive from a cold halo of material surrounding the hot core or hot cores (Hollis, private communication), as is the case with propenal (CH_2CHCHO) and propanal (CH_3CH_2CHO) (Hollis et al. 2004). Ketenimine appears to be somewhat of an exception, since it is found closer to the hot core with a rotational temperature of ≈65 K. It is unclear what type of model of interstellar chemistry should be applied to these detections, since the material can be thought of as either ambient or affected in some way by the hot core/massive star formation region. The chemistry of none of the three species recently detected towards Sgr B2(N) is in the current major reaction networks.

Ketenimine (CH_2CNH) was detected towards Sgr B2(N) with a column density of 1.5×10^{16} cm^{-2} by Lovas et al. (2006b), corresponding to a fractional abundance of $(0.1–3.0)\times10^{-9}$ with respect to H_2. They suggested that this molecule is likely formed by isomerization of methyl cyanide (CH_3CN) with energy supplied by shocks. Cyclopropenone (c-C_3H_2O) was detected towards this source by Hollis et al. (2006a) with a column density of $\approx1\times10^{13}$ cm^{-2}, corresponding to a fractional abundance with respect to H_2 of $\approx6\times10^{-11}$. Hollis et al. (2006a) maintained that since c-C_3H_2 is also present, it is possible that cyclopropenone can be formed from the simpler ring species by some type of oxygen addition. Finally, Hollis et al. (2006b) found another molecule, acetamide (CH_3CONH_2), towards the environs of Sgr B2(N) with a column density of 1.8×10^{14} cm^{-2}. They wrote that the exothermic reaction of formamide ($HCONH_2$) with the methylene radical (CH_2) could account for the synthesis of interstellar acetamide in the presence of shock phenomena, although radiative association reactions normally are fastest under low-energy conditions.

In this paper, we report a detailed look at the chemistry of these seven species undertaken to determine if they can be produced by gas-phase processes under ambient and quiescent cold cloud conditions. Although such conditions likely pertain to TMC-1, it is not clear that they do indeed pertain to even the colder portions of the envelope of Sgr B2(N). For the TMC-1 species, we incorporate some neutral-radical reactions to enhance the rate of formation of the species considered, of which three-quarters are already in our osu.01.2007 network, while for the Sgr B2(N) species, we must include these three molecules in our network for the first time. We do not include the molecules detected by Hollis et al. (2004) towards Sgr B2(N) – propenal (CH_2CHCHO) and propanal (CH_3CH_2CHO) – because these, especially the latter, bear the characteristics of saturated or nearly-saturated species formed on grain surfaces.

The remainder of the paper is divided as follows. In Sect. 2, we briefly describe the chemical reaction network used, and then discuss the adopted chemistry of each of the seven molecules. In Sect. 3, we present our modeling results and compare them with observational abundances. Section 4 contains our conclusions.

2. Molecules and synthesis

We started with the latest version of the gas-phase chemical reaction network, osu.01.2007, which contains 452 species and 4431 reactions (`http://www.physics.ohio-state.edu/~eric/research.html`). A molecular hydrogen density $n_H = 2\times10^4$ cm^{-3}, a temperature $T = 10$ K, a cosmic-ray ionization rate $\zeta = 1.3\times10^{-17}$ s^{-1}, and a visual extinction $A_V = 10$ mag were used for both TMC-1 and the cold halo around Sgr B2(N).

Table 1. Initial abundances.

Species	Sgr B2(N)	TMC-1
He	6.00×10^{-2}	6.00×10^{-2}
N	2.14×10^{-5}	2.14×10^{-5}
O	1.76×10^{-4}	6.10×10^{-5}
H_2	5.00×10^{-1}	5.00×10^{-1}
C^+	7.30×10^{-5}	7.30×10^{-5}
S^+	8.00×10^{-8}	8.00×10^{-8}
Si^+	8.00×10^{-9}	8.00×10^{-9}
Fe^+	3.00×10^{-9}	3.00×10^{-9}
Na^+	2.00×10^{-9}	2.00×10^{-9}
Mg^+	7.00×10^{-9}	7.00×10^{-9}
P^+	3.00×10^{-9}	3.00×10^{-9}
Cl^+	4.00×10^{-9}	4.00×10^{-9}
F^+	6.69×10^{-9}	6.69×10^{-9}
e^-	7.31×10^{-5}	7.31×10^{-5}

For the warmer region where ketenimine is detected we raised the temperature to 50 K. For Sgr B2(N), we used the standard low-metal elemental abundances (Graedel et. al 1982) while for TMC-1 we used carbon-rich elemental abundances (Wakelam et al. 2006). The initial abundances for both cases are listed in Table 1 with respect to the total hydrogen nuclei n_H. Reactions added to our network to treat the chemistry of the GBT molecules are listed in Table 2 (online only) along with their adopted rate coefficients k and references. This table also contains current reactions in the network pertaining to these species. For bimolecular reactions, the rate coefficients are parameterized by the expression $k = \alpha\times(T/300)^\beta\times\exp[-\gamma/T]$, whereas for cosmic-ray induced photodissociation, $k = \alpha\times\zeta$.

2.1. Molecules detected in TMC-1

To compute abundances for methyl cyanoacetylene and cyanoallene, we included their formation by neutral-radical reactions involving the radical CN and the hydrocarbons methyl acetylene (CH_3CCH) and allene (CH_2CCH_2). The former is a well-known interstellar molecule, while allene cannot be detected since it is nonpolar. These hydrocarbon isomers are not treated individually in our network; instead, we consider the sum of their abundances, labeled as a species C_3H_4, and add a parameter $\delta = [CH_3CCH]/[C_3H_4]$, which can be varied, for use in the chemical reaction network. The neutral-radical reactions have been studied via the CRESU technique (Carty et al. 2001) and found to have temperature-independent rate coefficients in the range 15–295 K of 4.1×10^{-10} cm^3 s^{-1}. A subsequent combined crossbeam and ab initio study (Balucani et al. 2002) found the products for these two reactions shown below:

$$CH_3CCH + CN \rightarrow CH_2CCHCN + H \quad (1)$$

$$CH_3CCH + CN \rightarrow CH_3CCCN + H \quad (2)$$

$$CH_2CCH_2 + CN \rightarrow CH_2CCHCN + H \quad (3)$$

$$CH_2CCH_2 + CN \rightarrow HCCCH_2CN + H \quad (4)$$

where the product ratio between cyanoallene and methyl cyanoacetylene in reactions (1) and (2) is 1:1 and that between cyanoallene and the third isomer, 3-cyano methylacetylene ($HCCCH_2CN$), in reactions (3) and (4) is 9:1. This third isomer has not yet been detected in the interstellar medium, possibly because 3-cyano methylacetylene ($HCCCH_2CN$) has a much smaller dipole moment than the other two isomers. If we label

the reaction rate coefficient for reactions $C_3H_4 + CN \rightarrow C_4H_3N + H$ to be k, the production rate of cyanoallene is $[0.5 \times \delta + 0.9 \times (1\text{-}\delta)] \times k$, while those for methyl cyanoacetylene and 3-cyano methylacetylene are $[0.5 \times \delta] \times k$ and $[0.1 \times (1\text{-}\delta)] \times k$ respectively.

In addition to the neutral-radical channels, the three isomers can be formed from ion-molecule channels, which lead initially to the production of a protonated ion precursor, $C_4H_4N^+$. Although the structural isomers of this ion are not known, to the best of our knowledge, we assume that when they undergo dissociative recombination leading to channels that form the three C_4H_3N isomers:

$$C_4H_4N^+ + e^- \rightarrow CH_2CCHCN + H \quad (5)$$

$$C_4H_4N^+ + e^- \rightarrow CH_3CCCN + H \quad (6)$$

$$C_4H_4N^+ + e^- \rightarrow HCCCH_2CN + H, \quad (7)$$

the relative rates of production of the isomers are the same as for the neutral-radical pathways. The argument is based on the assumption that the isomers of the ion are related in an intimate manner to those of the C_4H_3N isomers. Our calculations show that the neutral-radical channels are the more important. It should be noted that for all dissociative recombination reactions considered in this paper, branching fractions in which more than one H atom is removed are also included. After being produced, the neutral C_4H_3N molecules are destroyed via standard ion-molecule reactions with ions such as HCO^+, H_3^+, C^+ and He^+, as well as via photodissociation caused by cosmic-ray induced photons. Some of the ion-molecule reactions protonate the C_4H_3N species, which are reformed via dissociative recombination reactions with less than 100% efficiency since there are other product channels.

In the current network, methyl cyanodiacetylene (CH_3C_5N) is produced in one channel of the dissociative recombination of $C_6H_4N^+$:

$$C_6H_4N^+ + e^- \rightarrow CH_3C_5N + H. \quad (8)$$

To supplement its formation rate, we have added the neutral-radical reaction

$$CN + CH_3C_4H \rightarrow CH_3C_5N + H, \quad (9)$$

in analogy with the measured formation of methyl cyanoacetylene (Carty et al. 2001). For the rate coefficient of this reaction, we chose the same parameters as measured for $CN + CH_3CCH$ (Carty et al. 2001). Once produced, methyl cyanodiacetylene is destroyed by ion-molecule reactions and cosmic ray-induced photodissociation.

For the final GBT molecule observed in TMC-1, methyl triacetylene (CH_3C_6H), the current network contains only the synthesis via the dissociative recombination of the precursor ion $C_7H_5^+$:

$$C_7H_5^+ + e^- \rightarrow CH_3C_6H + H. \quad (10)$$

To this reaction, we have added the following neutral-radical reactions:

$$CCH + CH_3C_4H \rightarrow CH_3C_6H + H \quad (11)$$

$$C_6H + CH_4 \rightarrow CH_3C_6H + H. \quad (12)$$

The reaction involving the CCH radical is assumed to proceed at the same rate as the reaction between CCH and CH_3CCH, which has been studied in the laboratory by Carty et al. (2001). This reaction has also been added to the network. The reaction between C_6H and CH_4 is based on one between CCH and CH_4, which has only been studied at 300 K (Laufer & Fahr 2004), and has a rate somewhat below the standard neutral-radical value, possibly suggesting a small activation energy barrier. We assume here nevertheless that its rate coefficient is independent of temperature. In our calculations, the reaction is at least as important in the production of methyl triacetylene as that involving CCH. Once produced, methyl triacetylene is depleted by ion-molecule reactions, reaction with atomic carbon, and cosmic-ray-induced photodissociation.

2.2. Sgr B2 molecules

Ketenimine (CH_2CNH) is likely formed by the dissociative recombination of protonated acetonitrile, CH_3CNH^+, which also serves as a precursor for acetonitrile (CH_3CN) and the cyanomethyl radical:

$$CH_3CNH^+ + e^- \rightarrow CH_2CNH + H, \quad (13)$$

$$CH_3CNH^+ + e^- \rightarrow CH_3CN + H, \quad (14)$$

$$CH_3CNH^+ + e^- \rightarrow CH_2CN + H + H. \quad (15)$$

We assume that each channel is produced equally. If our assumption is correct, ketenimine should also be detectable in TMC-1 along with acetonitrile and cyanomethyl, since these species are detected there. Once produced, the ketenimine molecules can be destroyed by reactions with relatively abundant ions.

Deducing a reaction pathway for the formation of cyclopropenone (c-C_3H_2O) is less simple (Hollis et al. 2006a). Since the related species c-C_3H_2 is ubiquitous in the interstellar medium, it is natural to determine whether it can be a precursor to cyclopropenone through some reaction with an oxygen-containing species. Let us first consider the following neutral-neutral reactions:

$$c\text{-}C_3H_2 + O_2 \rightarrow c\text{-}C_3H_2O + O\ , \quad (16)$$

$$c\text{-}C_3H_2 + O \rightarrow c\text{-}C_3H_2O + h\nu, \quad (17)$$

$$c\text{-}C_3H_2 + OH \rightarrow c\text{-}C_3H_2O + H. \quad (18)$$

Of these three reactions, however, only that with the radical OH does not possess a barrier according to quantum chemical calculations (Talbi, private communication). What about ion-molecule pathways leading to the protonated precursor c-$C_3H_3O^+$, which can then undergo dissociative recombination to form cyclopropenone:

$$c\text{-}C_3H_3O^+ + e^- \rightarrow c\text{-}C_3H_2O + H? \quad (19)$$

The c-$C_3H_3O^+$ might be produced by various ion-neutral reactions between ions with a three-carbon cylic structure and oxygen-containing molecules/atoms such as:

$$c\text{-}C_3H_2^+ + H_2O \rightarrow c\text{-}C_3H_3O^+ + H, \quad (20)$$

$$c\text{-}C_3H_3^+ + O \rightarrow c\text{-}C_3H_2O^+ + H, \quad (21)$$

$$c\text{-}C_3H_2O^+ + H_2 \rightarrow c\text{-}C_3H_3O^+ + H, \quad (22)$$

$$c\text{-}C_3H_4^+ + O \rightarrow c\text{-}C_3H_3O^+ + H. \quad (23)$$

The first reaction of the four has been found not to occur at room temperature in the laboratory (Prodnuk et al. 1992), while the two step-synthesis starting from reaction (21) fails because the subsequent hydrogenation reaction is endothermic. Only reaction (23) remains a possible pathway to form protonated cyclopropenone starting from a three-membered ring, and this reaction has been added to our network. In addition, if the radiative association between $C_2H_3^+$ and CO to form an ion of the generic formula $C_3H_3O^+$, which is already in our network, produces a ring, protonated cyclopropenone is the result:

$$C_2H_3^+ + CO \rightarrow c\text{-}C_3H_3O^+ + h\nu. \quad (24)$$

The association reaction has, however, been studied in the three-body limit by Scott et al. (1995), who found the dominant product to be protonated propadienone (H_2CCHCO^+). These authors used their results to rule out reaction (24) as a source of protonated propynal, which would then lead to propynal, a known interstellar molecule actually detected towards Sgr B2(N) (Hollis et al. 2004). Cyclopropenone is destroyed by reactions with ions.

For the third detected molecule in the halo surrounding Sgr B2 (N), acetamide (CH_3CONH_2), Hollis et al. (2006b) suggested the main formation method might be the exothermic neutral-radical reaction between formamide and the methylene (CH_2) radical:

$$NH_2CHO + CH_2 \rightarrow CH_3CONH_2 + h\nu. \quad (25)$$

This reaction, however, involves a spin flip and thus probably an energy barrier. In addition, it is an association reaction, which must occur via radiative stabilization in the low-density interstellar medium. A more likely radiative association reaction involving formamide is the ion-molecule system

$$NH_2CHO + CH_3^+ \rightarrow CH_3CHONH_2^+ + h\nu, \quad (26)$$

which produces protonated acetamide. This species can then form acetamide by dissociative recombination:

$$CH_3CHONH_2^+ + e^- \rightarrow CH_3CONH_2 + H. \quad (27)$$

Because the rate coefficient for reaction (26) has not been calculated or measured, we assume that it possesses the large value of 1×10^{-9} cm^3 s^{-1} at 10 K. We also consider a second radiative association reaction, involving acetaldehyde (CH_3CHO) and the ammonium ion:

$$CH_3CHO + NH_4^+ \rightarrow CH_3CHONH_4^+ + h\nu, \quad (28)$$

which produces a large positive ion. This ion can, among other channels, produce acetamide upon dissociative recombination with electrons. Once again, we assume that the rate coefficient for this radiative association is large at 10 K. These and other radiative association reactions considered in this paper may well form product isomers not included here. If the reactions are found to be efficient in producing the desired species, then detailed calculations and or experiments will have to be undertaken to determine the actual rates and products formed. Acetamide is depleted by ion-molecule reactions.

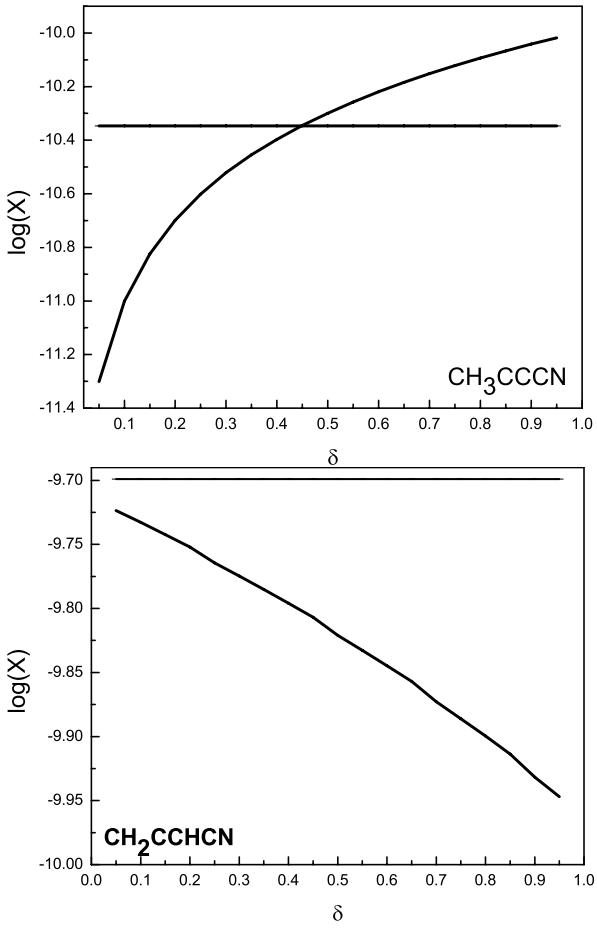

Fig. 1. Calculated fractional abundances X (with respect to H_2) at 1×10^5 yr plotted vs. the parameter δ (see text); *upper panel*, CH_3CCCN; *lower panel*, CH_2CCHCN. Observed values shown as horizontal lines.

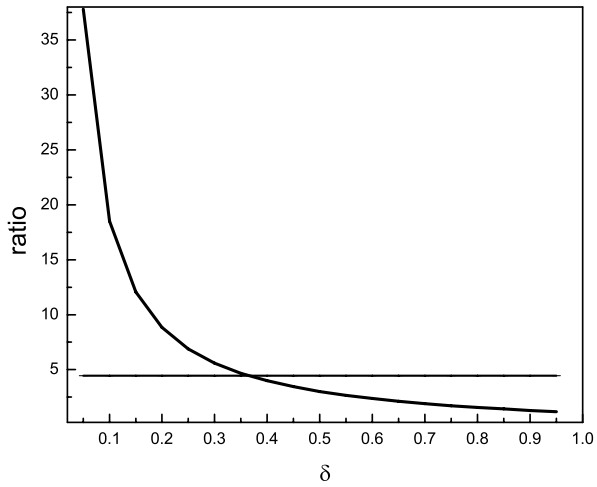

Fig. 2. Calculated abundance ratio of cyanoallene to methyl cyanoacetylene at $t = 1 \times 10^5$ yr plotted vs. parameter δ. Observed ratio of 4.5 plotted as horizontal line.

3. Results and discussion

3.1. TMC-1

Figure 1 shows calculated fractional abundances with respect to H_2 for the two observed isomers of C_4H_3N, methyl cyanoacetylene and cyanoallene, near their peak early-time values ($t = 1 \times 10^5$ yr) as a function of the parameter δ, which is the ratio of the abundance of methyl acetylene to the sum of the methyl acetylene and allene abundances. Also shown are the observed fractional abundances with respect to H_2 for methyl cyanoacetylene and cyanoallene, based on the column density results of Lovas et al. (2006a) and the assumption that the H_2 column density is 10^{22} cm^{-2}. It can be seen that at early-time the calculated

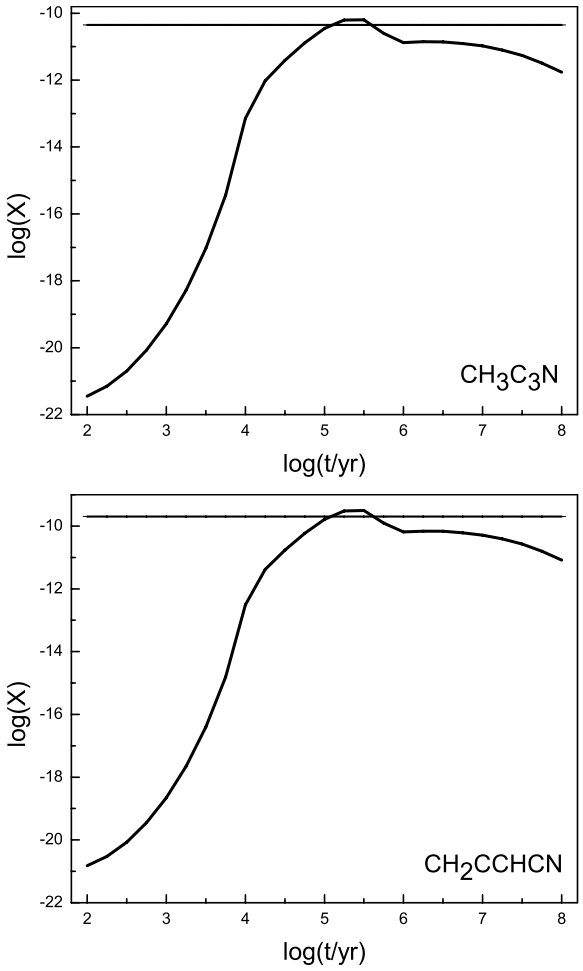

Fig. 3. Calculated fractional abundances of C_4H_3N isomers vs. time; *upper panel*, methyl cyanoacetylene (CH_3CCCN); *lower panel*, cyanoallene (CH_2CCHCN); $\delta = 0.35$. Observed abundances shown as horizontal lines.

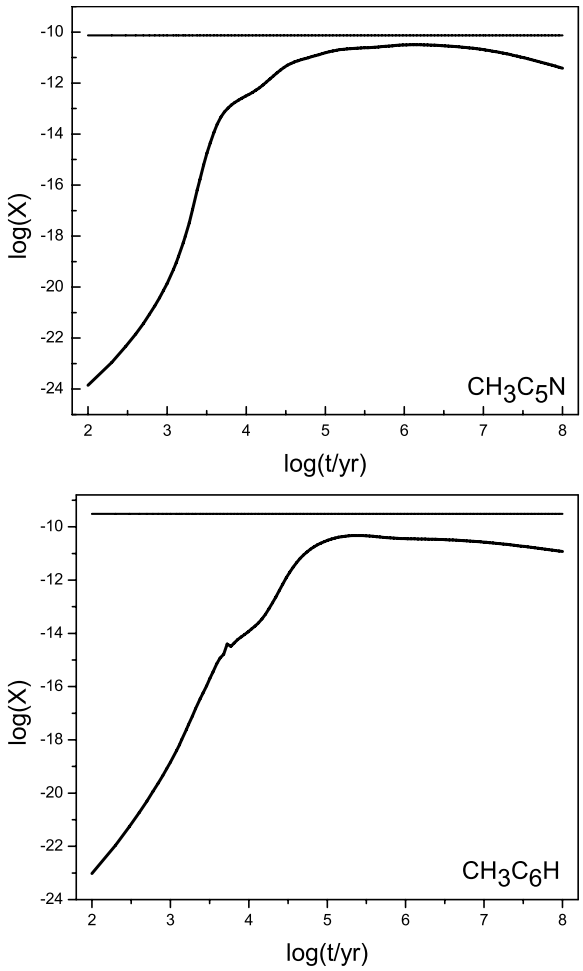

Fig. 4. Calculated fractional abundances of methyl cyanodiacetylene (CH_3C_5N) and methyl triacetylene (CH_3C_6H) plotted vs. time. Horizontal lines represent observed abundances.

abundance of cyanoallene is in reasonable agreement with observation for all values of δ. The worst agreement occurs as δ approaches unity, but even here the calculated abundance is low by a factor less than two. The role of δ is more important for the calculation of the methyl cyanoacetylene abundance; here the calculated abundance is almost an order of magnitude low when δ is near zero but increases rapidly with increasing δ. This result is reasonable because, as discussed previously, methyl acetylene is the main source of methyl cyanoacetylene. To obtain some sort of fit for the best value of δ, we can look at the calculated abundance ratio between cyanoallene and methyl acetylene at early-time, the observed value of which is 4.5. Figure 2 shows the calculated ratio plotted against δ; it can be seen that a value of 0.35 gives the best agreement with observation. Thus, we predict that the abundance of methyl acetylene is 0.35 and that of allene 0.65 of the overall C_3H_4 abundance. Or, put differently, the abundance of allene is almost double that of methyl acetylene.

With $\delta = 0.35$, we plot the calculated methyl cyanoacetylene and cyanoallene fractional abundances against time in Fig. 3. The similarity between the two figures stems from the fact that the molecules are produced from C_3H_4 isomers with a constant abundance ratio and destroyed in a similar fashion. It can be seen that the values peak at times slightly greater than 10^5 yr but are in excellent agreement with observation from 10^5 yr through 10^7 yr. Furthermore, the predicted abundance of the third isomer, 3-cyanomethylacetylene ($HCCCH_2CN$), is $\approx 1 \times 10^{-11}$ at early time, a value lower than those for methyl cyanoacetylene and cyanoallene by factors of $\approx$4 and $\approx$16, respectively.

The calculated fractional abundances of methyl cyanodiacetylene and methyl triacetylene are shown in Figure 4 as functions of time. Also plotted as horizontal lines are the observed fractional abundances of $\approx 8 \times 10^{-11}$ for methyl cyanodiacetylene (Snyder et al. 2006; Remijan et al. 2006) and 3×10^{-10} for methyl triacetylene (Remijan et al. 2006). As can be seen in the figure, the calculated abundance for methyl cyanodiacetylene is now in excellent agreement with observation from times starting at 10^5 yr. The synthesis involving the reaction between CN and CH_3C_4H is thus quite superior to the ion-molecule pathways, found totally inadequate by Snyder et al. (2006). The calculated abundance for methyl triacetylene is, however, in poorer agreement with the observation; values obtained at $\geq 2 \times 10^5$ yr are almost one order of magnitude too low. Nevertheless, the combined uncertainties in observed and calculated values will result in an overlap of Gaussian distributions if one assumes an observational uncertainty of a factor of three (up or down) and calculated uncertainties similar to those found for TMC-1 by Wakelam et al. (2006).

3.2. Halo of Sgr B2 (N)

Figure 5 shows the calculated fractional abundance of ketenimine (CH_2CNH) as a function of time as well as a gray area that depicts the range of observed abundances. The assumed temperature has been raised to 50 K from the 10 K appropriate to the cold halo, and the result is an increase of a factor of three in the peak calculated abundance. The early-time abundance at either temperature is well within the observed range, and so it appears that a standard gas-phase analysis at low temperature reproduces observation. Naturally, the calculated result is based solely on whether or not the dissociative recombination reaction between protonated acetonitrile and electrons has a significant channel that leads to CH_2CNH + H. Note that since oxygen-rich abundances are used, there is a sharp drop-off past early time for organic molecules such as ketenimine.

In complete contrast to the case of ketenimine, the cold gas-phase model fails for the case of acetamide (CH_3CONH_2). Compared with the observed fractional abundance of 1.1×10^{-9} (Hollis et al. 2006b), our peak calculated value is about six orders of magnitude too low. The huge discrepancy derives from the fact that our starting materials, formamide and acetaldehyde, themselves have small abundances. We attempted to boost the abundance of formamide (NH_2CHO) by including a possible radiative association reaction between NH_4^+ and H_2CO:

$$NH_4^+ + H_2CO \rightarrow NH_4CH_2O^+ + h\nu, \quad (29)$$

followed by dissociative recombination. The association reaction is known to occur under high-density conditions (Adams et al. 1980), but even with the assumption that the radiative association reaction has a very large rate coefficient, we do not produce much more formamide than without the reaction. If the problem lies in our underproduction of formamide, we can re-express the calculated abundance of acetamide in terms of that of formamide; at early time our predicted abundance ratio is 0.003. The observed abundance ratio in the cold halo region is 0.1–0.5 (Hollis et al. 2006b). So, it would appear that formamide is not the proper precursor in any event.

Finally, the case of cyclopropenone is somewhat ambiguous. If one assumes that the radiative association reaction between $C_2H_3^+$ and CO (Scott et al. 1995) does lead to protonated cyclopropenone, then a peak fractional abundance exceeding 10^{-10} for cyclopropenone is computed for early-time. This abundance compares favorably with the observed value of 6×10^{-11} (Hollis et al. 2006a). However, it is more likely that the dominant product of the radiative association is not the ring-closure product but instead protonated propadienone, so that the production rate of cyclopropenone via this route is at best ≈1–5% of the production rate of propadienone, which has not yet been detected in the interstellar medium (McEwan, private communication). In that case, the peak calculated fractional abundance lies well below the observed value. If we rule out the association reaction (reaction 24), there remain two other pathways: the neutral-radical reaction involving c-C_3H_2 and OH and the ion-molecule reaction between $C_3H_4^+$ and O. Given the low abundance of the $C_3H_4^+$ ion, the neutral-radical channel dominates but only leads to the production of a fractional abundance for cyclopropenone at early-time of 6×10^{-12}, which is an order of magnitude low. Given the difficulty of deducing the proper H_2 column density in this source as well as the uncertainty in the calculated abundance (Wakelam et al. 2006), the cold gas-phase production mechanism cannot be ruled out.

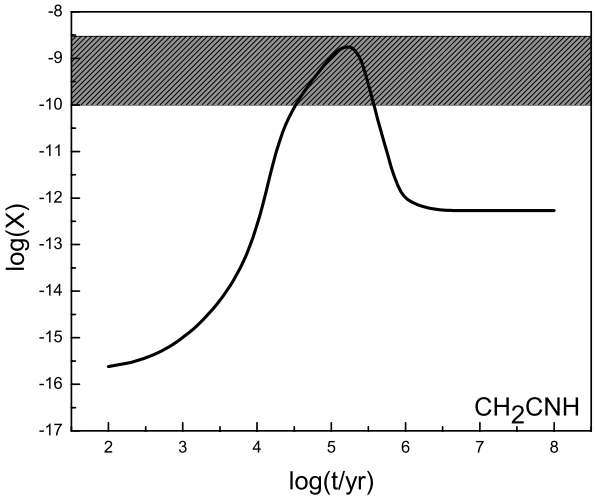

Fig. 5. Calculated fractional abundance of ketenimine plotted as a function of time. The shadowed region represents the range of observed values. The assumed temperature is 50 K.

4. Conclusions

Sgr B2(N) is a complex source with a core-halo type structure, from which organic molecules can be detected in absorption. Although such molecules may currently be existing under the cold conditions of the halo, it is certainly not clear where their origin was. Nevertheless, Occam's Razor suggests that one make the simplest assumption as an initial guess: the molecules are produced by gas-phase processes in the outer regions where they are detected. Only if this assumption fails should one go to more complex hypotheses. Unlike the case for the cold dark cloud core TMC-1, where the gas-phase model works tolerably well for those molecules either newly-detected or confirmed by the use of the GBT, the gas-phase model performs rather poorly for two of the the three new molecules detected towards Sgr B2(N). If one adds to this score the failure of gas-phase models to reproduce earlier observed abundances of propenal (CH_2CHCHO) and propanal (CH_3CH_2CHO) towards the same source (Hollis et al. 2004), one comes to the conclusion that most organic species towards Sgr B2(N) are formed at least partially on granular surfaces.

This assumption raises new problems; in particular, how do the molecules leave the grains in a cold region? One possibility is that non-thermal desorptive processes, such as desorption via the energy generated by exothermic chemical reactions on granular surfaces (Garrod et al. 2007), can lead to sufficient concentrations of these molecules (or their precursors) in the gas-phase. For the case of TMC-1, grain chemistry followed by non-thermal desorption is the only known manner in which gaseous methanol can be produced. Another possibility often invoked when discussing the galactic center region is that intermittent shock waves pervade the medium and sputter molecules off of grain surfaces. Yet a third possibility is that the molecules are formed in the warmer (hot core) region and then diffuse throughout the halo. The hot core gas-grain model of Garrod & Herbst (2006) only requires surface temperatures of 40 K or so for the production of organic molecules; in this model temperatures greater than 10 K are needed for radicals on grains to diffuse and react to form the larger species. Once these molecules are formed on a surface of 40 K or so, they can be desorbed by shock waves. To determine which if any of these alternative explanations are correct for Sgr B2(N) will require a deeper understanding of the

chemical and physical processes involved and more detailed observations of molecules surrounding hot-core sources.

Acknowledgements. We thank D. Talbi for her quantum chemical calculations regarding the formation of cyclopropenone, M. McEwan for information about the association reaction between $C_2H_3^+$ and CO, and J. M. Hollis for reading an earlier version of this manuscript. E. H. acknowledges the support of the National Science Foundation (US) for his research program in astrochemistry.

References

Adams, N. G., Smith, D., & Paulson, J. F. 1980, J. Chem. Phys., 72, 288
Adams, N. G., Babcock, L. M., Mostefaouoi, T. M., & Kerns, M. S. 2003, Int. J. Mass. Spectrom., 223, 459
Balucani, N., Asvany, O., Kaiser, R.-I., & Osamura, Y. 2002, J. Phys. Chem. A, 106, 4301
Carty, D., Le Page, V., Sims, I. R., & Smith, I. W. M. 2001, Chem. Phys. Lett., 344, 310
Chesnavich, W. J., Su, T., & Bowers, M. T. 1980, J. Chem. Phys., 72, 2641
Chin, Y., Kaiser, R. I., Lemme, C., & Henkel, C. 2006, in Astrochemistry, From Laboratory Studies to Astronomical Observations, AIP Conf. Proc., 855, 149
Garrod, R. T., & Herbst, E. 2006, A&A, 457, 927
Garrod, R. T., Wakelam, V., & Herbst, E. 2007, A&A, 467, 1103
Graedel, T. E., Langer, W. D., & Frerking, M. A. 1982, ApJS, 48, 321
Hollis, J. M., Jewell, P. R., Lovas, F. J., Remijan, A., & Møllendal, H. 2004, ApJ, 610, L21
Hollis, J. M., Remijan, A. J., Jewell, P. R., & Lovas, F. J. 2006a, ApJ, 642, 933
Hollis, J. M., Lovas, F. J., Remijan, A. J., et al. 2006b, ApJ, 643, L25
Laufer, A. H., & Fahr, A. 2004, Chem. Rev., 104, 2813
Lovas, F. J., Remijan, A. J., Hollis, J. M., Jewell, P. R., & Snyder, L. E. 2006a, ApJ, 637, L37
Lovas, F. J., Hollis, J. M., Remijan, A. J., & Jewell, P. R. 2006b, ApJ, 645, L137
Prodnuk, S. D., Gronert, S., Bierbaum, V. M., & DePuy, C. H. 1992, Org. Mass. Spectrom., 27, 416
Remijan, A. J., Hollis, J. M., Snyder, L. E., Jewell, P. R., & Lovas, F. J. 2006, ApJ, 643, L37
Schwahn, G., Schieder, R., Bester, M., & Winnewisser, G. 1986, J. Mol. Spectrosc., 116, 263
Scott, G. B. I., Fairley, D. A., Freeman, C. G., Maclagan, R. G. A. R., & McEwan, M. J. 1995, IJMSIP, 149/150, 251
Snyder, L. E., Wilson, T. L., Henkel, C., Jewell, P. R., & Walmsley, C. M. 1984, BAAS, 16, 959
Snyder, L. E., Hollis, J. M., Jewell, P. R., Lovas, F. J., & Remijan, A. 2006, ApJ, 647, 412
Wakelam, V., Herbst, E., & Selsis, F. 2006, A&A, 451, 551

Online Material

Table 2. Reactions involving GBT molecules and their protonated ions.

Reaction	α	β	γ	Ref.
$C_3H_4 + CN \rightarrow C_4H_3N + H$	4.10×10^{-10}	0	0	1
$C_4H_3N \rightarrow C_3N + CH_3$	1.50×10^{3}	0	0	2
$C_4H_3N + H_3^+ \rightarrow C_4H_4N^+ + H_2$	1.08×10^{-8}	–0.5	0	2
$C_4H_3N + HCO^+ \rightarrow C_4H_4N^+ + CO$	4.11×10^{-9}	–0.5	0	2
$C_4H_3N + He^+ \rightarrow CH_3^+ + C_3N + He$	9.49×10^{-9}	–0.5	0	2
$C_4H_3N + H^+ \rightarrow CH_3^+ + HC_3N$	1.85×10^{-8}	–0.5	0	2
$C_4H_3N + C^+ \rightarrow C_2H_3^+ + C_3N$	2.90×10^{-9}	–0.5	0	2
$C_4H_3N + C^+ \rightarrow C_4H_3^+ + CN$	2.90×10^{-9}	–0.5	0	2
$C_4H_3N^+ + H_2 \rightarrow C_4H_4N^+ + H$	1.00×10^{-9}	0	0	2
$C_4H_5^+ + N \rightarrow C_4H_4N^+ + H$	1.00×10^{-10}	0	0	2
$CH_3^+ + HC_3N \rightarrow C_4H_4N^+ + h\nu$	8.60×10^{-11}	–1.4	0	2
$C_4H_4N^+ + C \rightarrow C_5H_3N^+ + H$	1.00×10^{-9}	0	0	2
$C_4H_4N^+ + e^- \rightarrow C_4H_3N + H$	1.00×10^{-6}	–0.3	0	2
$C_4H_4N^+ + e^- \rightarrow CH_3 + HC_3N$	1.00×10^{-6}	–0.3	0	2
$CH_3C_4H + CN \rightarrow CH_3C_5N + H$	4.10×10^{-10}	0	0	1, 3
$CH_3C_5N \rightarrow C_5N + CH_3$	1.50×10^{3}	0	0	2
$CH_3C_5N + C^+ \rightarrow C_6H_3^+ + CN$	6.24×10^{-9}	–0.5	0	2
$CH_3C_5N + H^+ \rightarrow CH_3^+ + HC_5N$	2.03×10^{-8}	–0.5	0	2
$CH_3C_5N + He^+ \rightarrow CH_3^+ + C_5N + He$	1.04×10^{-8}	–0.5	0	2
$CH_3C_5N + H_3^+ \rightarrow C_6H_4N^+ + H_2$	1.19×10^{-8}	–0.5	0	2
$CH_3C_5N + HCO^+ \rightarrow C_6H_4N^+ + CO$	4.34×10^{-9}	–0.5	0	2
$C_6H_5^+ + N \rightarrow C_6H_4N^+ + H$	1.00×10^{-10}	0	0	2
$CH_3^+ + HC_5N \rightarrow C_6H_4N^+ + h\nu$	8.60×10^{-11}	–1.4	0	2
$C_6H_4N^+ + C \rightarrow C_7H_3N^+ + H$	1.00×10^{-9}	0	0	2
$C_6H_4N^+ + e^- \rightarrow CH_3 + HC_5N$	1.00×10^{-6}	–0.3	0	2
$C_6H_4N^+ + e^- \rightarrow CH_3C_5N + H$	1.00×10^{-6}	–0.3	0	2
$CCH + CH_3C_4H \rightarrow CH_3C_6H + H$	1.80×10^{-10}	0	0	1,3
$C_6H + CH_4 \rightarrow CH_3C_6H + H$	7.00×10^{-12}	0	0	3
$C_7H_5^+ + e^- \rightarrow CH_3C_6H + H$	3.50×10^{-7}	–0.5	0	2
$C_7H_5^+ + e^- \rightarrow C_7H_2 + H_2 + H$	3.50×10^{-7}	–0.5	0	2
$C_2H_4^+ + C_5H_2 \rightarrow C_7H_5^+ + H$	5.52×10^{-10}	–0.5	0	2
$C_4H_2^+ + C_3H_4 \rightarrow C_7H_5^+ + H$	6.42×10^{-10}	–0.5	0	2
$C_4H_3^+ + C_3H_3 \rightarrow C_7H_5^+ + H$	1.65×10^{-9}	–0.5	0	2
$C_5H_2^+ + C_2H_4 \rightarrow C_7H_5^+ + H$	5.00×10^{-10}	0	0	2
$C_6H_2^+ + CH_4 \rightarrow C_7H_5^+ + H$	8.00×10^{-10}	0	0	2
$C_3H_3^+ + C_4H_2 \rightarrow C_7H_5^+ + h\nu$	1.00×10^{-13}	–2.5	0	2
$C_5H_3^+ + C_2H_2 \rightarrow C_7H_5^+ + h\nu$	1.00×10^{-9}	0	0	3
$C_7H_5^+ + N \rightarrow C_7H_3N^+ + H_2$	1.00×10^{-10}	0	0	2
$CH_3C_6H \rightarrow C_6H + CH_3$	1.50×10^{3}	0	0	2
$CH_3C_6H + C^+ \rightarrow C_7H_3^+ + CH$	9.00×10^{-10}	–0.5	0	2
$CH_3C_6H + C^+ \rightarrow C_8H_2^+ + H_2$	9.00×10^{-10}	–0.5	0	2
$CH_3C_6H + H^+ \rightarrow C_7H_3^+ + H_2$	2.92×10^{-9}	–0.5	0	2
$CH_3C_6H + H^+ \rightarrow C_7H_4^+ + H$	2.92×10^{-9}	–0.5	0	2
$CH_3C_6H + He^+ \rightarrow C_7H_2^+ + H_2 + He$	1.49×10^{-9}	–0.5	0	2
$CH_3C_6H + He^+ \rightarrow C_7H_3^+ + H + He$	1.49×10^{-9}	–0.5	0	2
$CH_3C_6H + H_3^+ \rightarrow C_7H_5^+ + H_2$	3.40×10^{-9}	–0.5	0	2
$CH_3C_6H + HCO^+ \rightarrow C_7H_5^+ + CO$	1.25×10^{-9}	–0.5	0	2
$CH_3C_6H + C \rightarrow C_8H_2 + H_2$	7.40×10^{-10}	0	0	2
$CH_3CNH^+ + e^- \rightarrow CH_2CNH + H$	1.00×10^{-7}	–0.5	0	3
$CH_2CNH + C^+ \rightarrow C_2H_3^+ + CN$	1.83×10^{-9}	–0.5	0	4
$CH_2CNH + H^+ \rightarrow CH_2CN^+ + H_2$	2.82×10^{-9}	–0.5	0	4
$CH_2CNH + H^+ \rightarrow CH_3CN^+ + H$	2.82×10^{-9}	–0.5	0	4
$CH_2CNH + He^+ \rightarrow CN^+ + CH_3 + He$	2.02×10^{-9}	–0.5	0	4
$CH_2CNH + He^+ \rightarrow CH_3^+ + CN + He$	2.02×10^{-9}	–0.5	0	4

Table 2. continued.

Reaction	α	β	γ	Ref.
$CH_2CNH + H_3^+ \rightarrow CH_3CNH^+ + H_2$	3.33×10^{-9}	–0.5	0	4
$CH_2CNH + HCO^+ \rightarrow CH_3CNH^+ + CO$	1.35×10^{-9}	–0.5	0	4
$HCN + CH_3^+ \rightarrow CH_3CNH^+ + h\nu$	9.00×10^{-9}	–0.5	0	2
$CH_3CNH^+ + e^- \rightarrow CH_2CN + H + H$	1.00×10^{-7}	–0.5	0	3
$CH_3CNH^+ + e^- \rightarrow CH_3CN + H$	1.00×10^{-7}	–0.5	0	3
$CH_3CN + H_3^+ \rightarrow CH_3CNH^+ + H_2$	9.10×10^{-9}	–0.5	0	2
$CH_3CN + HCO^+ \rightarrow CH_3CNH^+ + CO$	3.70×10^{-9}	–0.5	0	2
$CH_3CN + H_3O^+ \rightarrow CH_3CNH^+ + H_2O$	4.22×10^{-9}	–0.5	0	2
$CH_3CN + HOCO^+ \rightarrow CH_3CNH^+ + CO_2$	3.28×10^{-9}	–0.5	0	2
$c\text{-}C_3H_2 + OH \rightarrow c\text{-}C_3H_2O + H$	1.00×10^{-11}	0	0	5
$c\text{-}C_3H_4^+ + O \rightarrow c\text{-}C_3H_3O^+ + H$	2.00×10^{-10}	0	0	6
$C_2H_3^+ + CO \rightarrow c\text{-}C_3H_3O^+ + h\nu$	2.00×10^{-16}	–2.5	0	7
$c\text{-}C_3H_3O^+ + e^- \rightarrow c\text{-}C_3H_2O + H$	1.00×10^{-7}	–0.5	0	3
$c\text{-}C_3H_3O^+ + e^- \rightarrow C_2H_3 + CO$	1.00×10^{-7}	–0.5	0	3
$c\text{-}C_3H_2O + H_3^+ \rightarrow c\text{-}C_3H_3O^+ + H_2$	1.01×10^{-8}	–0.5	0	4
$c\text{-}C_3H_2O + HCO^+ \rightarrow c\text{-}C_3H_3O^+ + CO$	3.91×10^{-9}	–0.5	0	4
$c\text{-}C_3H_2O + H_3O^+ \rightarrow c\text{-}C_3H_3O^+ + H_2O$	4.29×10^{-9}	–0.5	0	4
$c\text{-}C_3H_2O + He^+ \rightarrow C_3H_2^+ + O + He$	1.22×10^{-8}	–0.5	0	4
$c\text{-}C_3H_2O + H^+ \rightarrow C_3H_2^+ + OH$	1.71×10^{-8}	–0.5	0	4
$c\text{-}C_3H_2O + C^+ \rightarrow C_3H_2^+ + CO$	5.41×10^{-9}	–0.5	0	4
$NH_2CHO + CH_3^+ \rightarrow CH_3CHONH_2^+ + h\nu$	1.00×10^{-9}	0	0	3
$CH_3CHONH_2^+ + e^- \rightarrow CH_3CONH_2 + H$	1.00×10^{-7}	–0.5	0	3
$CH_3CHONH_2^+ + e^- \rightarrow CH_3 + NH_2CHO$	1.00×10^{-7}	–0.5	0	3
$CH_3CHO + NH_4^+ \rightarrow CH_3CHONH_4^+ + h\nu$	1.00×10^{-13}	–3.0	0	8
$CH_3CHONH_4^+ + e^- \rightarrow CH_3CONH_2 + H_2 + H$	1.00×10^{-7}	–0.5	0	3
$CH_3CHONH_4^+ + e^- \rightarrow CH_3 + NH_2CHO + H_2$	1.00×10^{-7}	–0.5	0	3
$CH_3CONH_2 + C^+ \rightarrow CH_3CONH_2^+ + C$	4.60×10^{-9}	–0.5	0	4
$CH_3CONH_2 + H^+ \rightarrow CH_3CONH_2^+ + H$	1.47×10^{-8}	–0.5	0	4
$CH_3CONH_2 + He^+ \rightarrow CH_3CONH_2^+ + He$	5.20×10^{-9}	–0.5	0	4
$CH_3CONH_2 + He^+ \rightarrow CH_3^+ + CO + NH_2 + He$	5.20×10^{-9}	–0.5	0	4
$CH_3CONH_2 + H_3^+ \rightarrow CH_3CHONH_2^+ + H_2$	8.60×10^{-9}	–0.5	0	4
$CH_3CONH_2 + HCO^+ \rightarrow CH_3CHONH_2^+ + CO$	3.30×10^{-8}	–0.5	0	4
$CH_3CONH_2^+ + H_2 \rightarrow CH_3CHONH_2^+ + H$	1.00×10^{-9}	0	0	3
$CH_3CONH_2^+ + e^- \rightarrow CH_3 + NH_2 + CO$	1.50×10^{-7}	–0.5	0	3

NOTE : The parameter α is in units of $cm^3\ s^{-1}$ for bimolecular reactions and is unitless for cosmic ray processes. [1] Ref. Carty et al. (2001); [2] osu.01.2007; [3] estimation according to analogous reaction rates; [4] calculation based on method of Chesnavich et al. (1980); [5] Ref. D. Talbi, private communication; [6] Ref. Prodnuk et al. (1992); [7] Ref. Scott et al. (1995); [8] Ref. Adams et al. (2003).